SLAC-PUB-2240
December 1978
(M)

TWO-PHOTON COLLISIONS AND SHORT-DISTANCE TESTS OF QUANTUM CHROMODYNAMICS*

Stanley J. Brodsky
Stanford Linear Accelerator Center
Stanford University, Stanford, California 94305

I. Introduction

I am very honored to speak today at this memorial for Joe Weis. Joe was strongly interested in photon-photon collisions as a new test of short-distance hadron dynamics, and it was a great pleasure for me to be able to work with him on this project. Although much of this field was novel to him, Joe mastered it very quickly, and his physics insights and computations formed a main core of our work with Tom DeGrand and Jack Gunion.[1] In this talk I will review the physics of two-photon collisions in $e^{\pm}$ storage rings with emphasis on the predictions of perturbative quantum chromodynamics for high transverse momentum reactions. Because of the remarkable scaling properties predicted by the theory, two-photon collisions may provide one of the cleanest tests of the QCD picture of short distance hadron dynamics. In order to contrast these predictions for photon-induced reactions with those for incident hadrons, I will also discuss predictions from QCD for hadron structure functions and form factors at large momentum transfer.

The photon plays a unique role in strong interaction dynamics because of its elementarity and its direct interactions with the hadronic constituents. Although it is well-known that highly virtual photons have asymptotically scale-free interactions with the quark current in QCD, it is perhaps not sufficiently emphasized that the interactions of real on-shell photons also become dominantly pointlike in large momentum transfer (short-distance) processes. The predictions by Bjorken and Paschos[2] for deep inelastic Compton scattering, and dimensional counting predictions[3] for exclusive and inclusive processes involving real photons are all based on the existence of direct $\gamma q\bar{q}$ perturbative couplings, and imply the breakdown of the vector meson dominance description[4] of the photon's hadronic interactions at short-distances and large momentum transfer. As a general rule, VMD can only be valid in QCD for low momentum transfer, nearly on-

* Work supported by the Department of Energy under contract number EY-76-C-03-0515.

(Presented at the Joseph M. Weis Memorial Symposium on Strong Interactions, University of Washington, Seattle, November 30, 1978.)

mass-shell processes where perturbation theory in α_s is invalid. Whenever a photon couples to far-off shell quarks (as in $\gamma q \to \gamma q$) the net real and virtual gluon radiative corrections are of order $\alpha_s(p_T^2) \sim O(\log^{-1}(p_T^2/\Lambda^2))$, and the point-like Born amplitude are expected to dominate in the asymptotic limit.

II. Photon-Photon Collisions

The production of hadrons in the collisions of two photons should provide an ideal laboratory for testing many features of the photon's hadronic interactions, including its short distance aspects. It is well known that photon-photon inelastic collisions in e^+e^- storage rings become an increasingly important source of hadrons as the center-of-mass energy $\sqrt{s} = 2E_e$ is raised.[5] The dominant part of the cross section for $e^+e^- \to e^+e^-$ + hadrons arises from the annihilation of two nearly on-shell photons emitted at small angles to the beam (see Fig. 1). The resulting cross section increases logarithmically with energy $\left(m_e^2/s \to 0,\ s >> m_H^2\right)$:

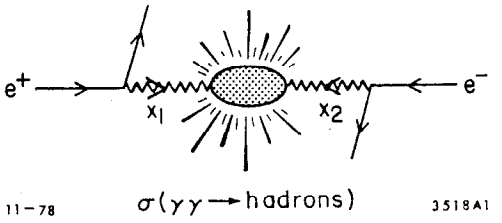

Fig. 1. Two-photon annihilation into hadrons in e^+e^- collisions.

$$d\sigma_{e^+e^- \to e^+e^- X}(s)/dm_H^2 \simeq \frac{\alpha^2}{\pi^2} \log^2\left(\frac{s}{m_e^2}\right) \frac{\sigma_{\gamma\gamma}(m_H^2)}{m_H^2} \log\left(\frac{s}{m_H^2}\right) \qquad (1)$$

where m_H is the invariant mass of the produced hadronic system. In contrast, the e^+e^- annihilation cross section decreases quadratically with energy. For example, at the beam energy of $E_e = 15$ GeV, the standard vector dominance estimate for $\sigma_{\gamma\gamma}(m_H^2)$ gives $\sigma(e^+e^- \to e^+e^-$ hadrons$) \simeq 15$ nb for $m_H \geq 1$ GeV, compared to the annihilation cross section $\sigma_{e^+e^- \to \gamma \to \text{hadrons}} \equiv R\sigma_{e^+e^- \to \gamma \to \mu^+\mu^-} \simeq (0.1\text{ nb})R$.

The event rate can be large because of (1) the relatively large efficiency for an electron to emit a photon: $\left(x \equiv (k_0 + k_3)/(p_0 + p_3) \simeq \omega/E\right)$

$$x\, G_{\gamma/e}(x) = x \frac{dN_{\gamma/e}}{dx} \simeq \left(\frac{\alpha}{2\pi} \log \frac{s}{m_e^2}\right)\left(1 + (1-x)^2\right)$$

$$\simeq .051 \quad (\sqrt{s} = 30 \text{ GeV},\ x \to 0) \qquad (2)$$

(2) the factor of log s/m_H^2 from the integration over the nearly flat rapidity distribution of the produced hadronic system, and (3) the fact that the cross section is dominated by low-mass hadronic states. For untagged leptons, the cross section for ee → eeX in the equivalent photon spectrum takes the general form[6]

$$d\sigma_{e^+e^- \to e^+e^- X}(s,t,u) = \int_0^1 dx_1 \int_0^1 dx_2 \, G_{\gamma/e}(x_1) \, G_{\gamma/e}(x_2) \times d\sigma_{\gamma\gamma \to X}(\hat{s} = x_1 x_2 s, \; \hat{t} = x_1 t, \; \hat{u} = x_2 u) \qquad (3)$$

where $G_{\gamma/e}(x)$ is the equivalent photon energy spectrum and $d\sigma_{\gamma\gamma \to X}$ is the differential cross section for the scattering of two oppositely directed unpolarized photons (of energy $x_1\sqrt{s}/2$, $x_2\sqrt{s}/2$ in the e^+e^- c.m. system) into a final state X. If the scattered lepton kinematics are measured, then the photon momenta are determined and the full range of hadronic $\gamma\gamma$ physics analogous to pp colliding ring physics becomes accessible.

A large-scale experimental investigation of two-photon physics is now planned at PEP and PETRA. Among the areas of interest are[7]

(a) the production of heavy leptons[8] ($\gamma\gamma \to \tau^+\tau^-$, etc.)

(b) The production of even charge conjugation states and hadronic resonances ($\gamma\gamma \to \eta_c$, etc.).

(c) The measurement of the total $\sigma_{\gamma\gamma}(s)$ cross section, including heavy quark thresholds.

(d) Measurements of the $\pi - \pi$ and $K^+ - K^-$ phase shifts via $\gamma\gamma \to M\bar{M}$ and unitarity, as well as checks of dimensional-coupling scaling laws for the crossed Compton amplitude at large s and t.

(e) Deep inelastic scattering on a photon target,[9] via electrons or positrons tagged at large momentum transfer $e\gamma \to e'X$.

In each case the spacelike mass of each photon can be individually tuned by tagging the scattered $e^\pm$. The photon linear polarization is determined by the lepton scattering plane. We also note that the $e^\pm$ circular polarization of an incident lepton is transferred to the emitted photon with 100% efficiency as $x_\gamma \to 1$.

III. Large p_T Processes

Perhaps the most interesting application of two photon physics is the production of hadrons and hadronic jets at large p_T. The elementary reaction $\gamma\gamma \to q\bar{q} \to$ hadrons yields an asymptotically scale-invariant two-jet cross section at large p_T proportional to the fourth power of the quark charge. The $\gamma\gamma \to q\bar{q}$ subprocess[10] implies the production of two non-colinear, roughly coplanar high p_T (SPEAR-like) jets, with a cross section nearly flat in rapidity. Such "short jets" will be readily distinguishable from $e^+e^- \to q\bar{q}$ events due to missing visible energy, even without tagging the forward leptons. It is most useful to determine the ratio,

$$R_{\gamma\gamma} \equiv \frac{d\sigma(e^+e^- \to e^+e^-q\bar{q} \to e^+e^- + \text{jets})}{d\sigma(e^+e^- \to e^+e^-\mu^+\mu^-)} \qquad (4)$$

since experimental uncertainties due to tagging efficiency and the equivalent photon approximation tend to cancel. In QCD, with 3-colors, one predicts[1]

$$R_{\gamma\gamma} = 3 \sum_{q=u,d,s,c,\ldots} e_q^4 \left(1 + 0\left[\frac{\alpha_s(4p_T^2)}{\pi}\right]\right) \qquad (5)$$

where p_T is the total transverse momentum of the jet (or muon) and $\alpha_s(Q^2) \to 1/(b \log Q^2/\Lambda^2)$, $4\pi b = 11 - 2/3\ n_f$ for n_f flavors. Measurements of the two-jet cross section and $R_{\gamma\gamma}$ will directly test the scaling of the quark propagator $\not{p}^{-1}$ at large momentum transfer, check the color factor [11] and the quark fractional charge. The QCD radiative corrections are expected to depend on the jet production angle and acceptance. Such corrections are of order $\alpha_s(p_T^2)$ since there are neither infrared singularities in the inclusive cross section, nor quark mass singularities at large p_T to give compensating logarithmic factors. The onset of charm and other quark thresholds can be studied once again from the perspective of $\gamma\gamma$-induced processes. The cross section for the production of jets with total hadronic transverse momentum ($p_T > p_{T\min}$) from the $\gamma\gamma \to q\bar{q}$ subprocess alone can be estimated from the convenient formula,[1,12]

$$\sigma_{e^+e^- \to e^+e^- \text{ Jet}+X}(s, p_T^{\text{jet}} > p_T^{\min}) \equiv R_{\gamma\gamma}\, \sigma_{e^+e^- \to e^+e^- \mu^\pm \mu^\mp}(s, p_T^{\mu^\pm} > p_T^{\min})$$

$$\simeq R_{\gamma\gamma} \frac{32\pi\alpha^2}{3} \left(\frac{\alpha}{2\pi} \log \frac{s}{m_e^2} \right)^2 \frac{\left(\log \frac{s}{p_{T\min}^2} - \frac{19}{6} \right)}{p_{T\min}^2}$$

$$\simeq \frac{0.5 \text{ nb GeV}^2}{p_{T\min}^2} \quad \text{at} \quad \sqrt{s} = 30 \text{ GeV} \quad . \qquad (6)$$

where we have taken $R_{\gamma\gamma} = 3\sum_q e_q^4 = 34/27$ above the charm threshold. For $p_{T\min} = 4$ GeV, $\sqrt{s} = 30$ GeV, this is equivalent to 0.3 of unit of R; i.e., 0.3 times the $e^+e^- \to \mu^+\mu^-$ rate. We note that at $\sqrt{s} = 200$ GeV, the cross section from the $e^+e^- \to e^+e^- q\bar{q}$ subprocess with $p_{T\min} = 10$ GeV is 0.02 nb, i.e.: about 9 units of R! At such energies e^+e^- colliding beam machines are more nearly laboratories for $\gamma\gamma$ scattering then they are for e^+e^- annihilation! A useful graph [12] of the increase in R from the $\gamma\gamma \to q\bar{q}$ process for various $x_{T\min} = 2p_{T\min}/\sqrt{s}$ is shown in Fig. 2. The $\log s/p_{T\min}^2 - 19/6$ in Eq. (6) arises from integration over the nearly flat rapidity distribution of the $\gamma\gamma$ system. The final state in high p_T $\gamma\gamma \to q\bar{q}$ events in the $\gamma\gamma$ center of mass should be very similar in multiplicity and other hadronic properties as $e^+e^- \to \gamma^* \to q\bar{q}$, although $u\bar{u}$ and $c\bar{c}$ events should be enhanced relative to $d\bar{d}$ and $s\bar{s}$ due to the e_q^4 dependence. Monte Carlo studies of SPEAR events at $s = 4p_T^2$ distributed uniformly in rapidity would be useful in order to learn how to identify and trigger $\gamma\gamma \to q\bar{q}$ events.

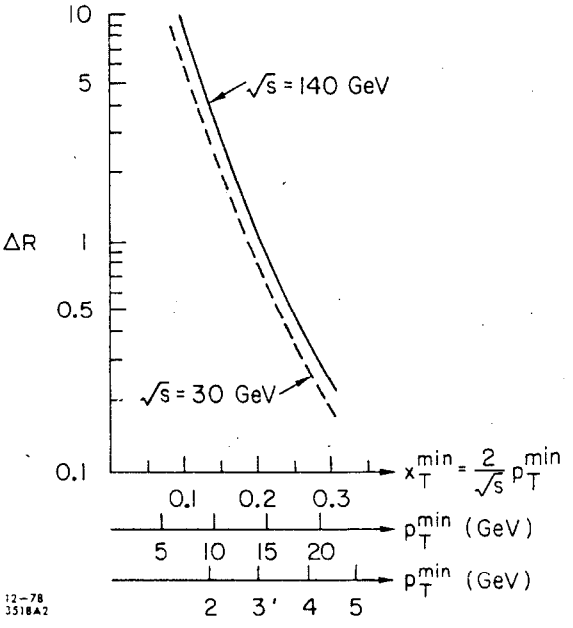

Fig. 2. The contribution to R from $\gamma\gamma \to q\bar{q}$ two jet processes at $\sqrt{s} = 30$ and 140 GeV (From Ref. 12).

Although the above prediction for $R_{\gamma\gamma}$ is one of the most straightforward consequences of perturbative QCD, it

should be noted that from the perspective of photon physics of 10 years ago, the occurence of events with the structure $\gamma\gamma \to$ jet + jet at high p_T could only be regarded as revolutionary. From the VMD standpoint, a real photon acts essentially as a sum of vector mesons; however, it is difficult to imagine an inelastic collision of two hadrons producing two large p_T jets without hadronic energy remaining in the beam direction!

On the other hand, if the $\gamma\gamma \to$ two jet events are not seen at close to the predicted magnitude with an approximately scale invariant cross section, then it would be hard to understand how the perturbative structure of QCD could be applicable to hadronic physics. In particular, unless the pointlike couplings of real photons to quarks are confirmed, then the analogous predictions for perturbative high p_T processes, involving gluons such as $gg \to q\bar{q}$ are probably meaningless.

IV. Multi-Jet Processes and the Photon Structure Function

In addition to the two-jet processes, QCD also predicts 3- and 4-jet events from subprocesses such as $\gamma q \to gq$ (3 jet production where one photon interacts with the quark constituent of the other photon) as well as the conventional high p_T QCD subprocesses $qq \to qq$ and $q\bar{q} \to gg$ (which lead to jets down the beam direction plus jets at large p_T)(see Fig. 3). The structure of these events are very similar to that for hadron-hadron collisions. The cross section for $Ed\sigma/d^3p_J$ ($\gamma\gamma \to$ jet + X or ee $\to$ ee jet + X) can be computed in the standard way from the hard scattering expansion ($\hat{s} = x_a x_b s$, etc.) [13]

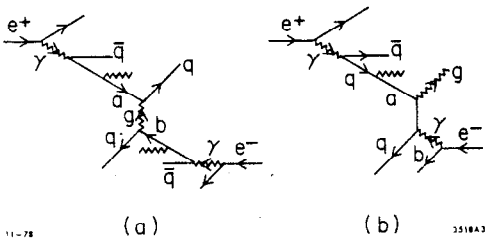

Fig. 3. Contributions from QCD subprocesses to (a) 4 jet and (b) 3 jet final states.

$$E\frac{d\sigma}{d^3p}(AB \to CX) \tilde{=} \sum_{abd} \int_0^1 dx_a \int_0^1 dx_b \, G_{a/A}(x_a) \, G_{b/B}(x_b)$$

$$\frac{d\sigma}{d\hat{t}}(ab \to cd)\Big|_{\hat{s},\hat{t},\hat{u}} \frac{\hat{s}}{\pi} \delta(\hat{s}+\hat{t}+\hat{u}) \qquad (7)$$

where the hard scattering occurs in $ab \to cd$ and the fragmentation function $G_{a/A}(x_a)$ gives the probability of finding constituent a with light-cone fraction $x_a = (p_a^0 + p_a^3)/(p_A^0 + p_A^3)$. In general, $G_{a/A}$ has a scale-breaking dependence on $\log p_T^2$ which arises from the constituent transverse momentum integration when gluon bremsstrahlung or pair production is involved.[14]

However, there is an extraordinary difference between photon and hadron induced processes. In the case of proton-induced reactions, $G_{q/p}(x,Q^2)$ is determined from experiment, especially deep inelastic lepton scattering. In the case of the photon, the $G_{q/\gamma}$ structure function required in Eq. (7) has a perturbative component which can be predicted from first principles in QCD. This component, as first computed by Witten,[15] has the asymptotic form at large probe momentum Q^2

$$G_{q/\gamma}(x,Q^2) \Longrightarrow \frac{\alpha}{\alpha_s(Q^2)} f(x) + O(\alpha^2) \qquad (8)$$

i.e.: aside from an overall logarithmic factor, the $\gamma \to q$ distribution Bjorken scales; $f(x)$ is a known, calculable function. Unlike the proton structure function which contracts to $x = 0$ at infinite probe momentum $Q^2 \to \infty$, this component of the photon structure function increases as $\log Q^2$ independent of x. This striking fact is of course due to the direct $\gamma \to q\bar{q}$ perturbative component in the photon wavefunction. (The apparent violation of momentum conservation when $\alpha_s(Q^2) < \alpha$ should be cured when higher order terms in α are taken into account.) In addition to the perturbative component, one also expects a nominal hadronic component due to intermediate vector meson states.

The calculation of the photon structure function is straightforward if we keep only leading logarithms in each order of perturbation theory. The leading contribution can be written as a simple convolution: (see Fig. 4)[14]

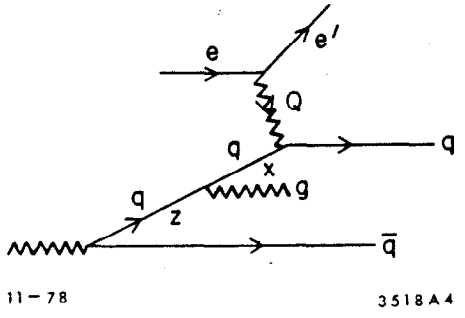

Fig. 4. Representation of the QCD photon structure function in deep inelastic scattering on a photon target. Real and virtual gluon corrections to all orders are included in the analytic results.

$$G_{q/\gamma}(x,Q^2) = \frac{3\alpha}{2\pi} e_q^2 \int_{\mu^2}^{Q^2} \frac{dk^2}{k^2} \int_x^1 \frac{dz}{z} \left[z^2 + (1-z)^2\right] G_{q/q}\left(\frac{x}{z}, Q^2, k^2\right) \quad (9)$$

where $G_{q/q}(x/z, Q^2, k^2)$ is the standard non-singlet distribution due to gluon bremsstrahlung for quarks in a target quark of mass k^2 being probed at four-momentum squared Q^2. The factor of 3 includes the sum over quark colors. In addition one can include smaller sea quark contributions form $g \to q\bar{q}$ processes. The region $k^2 < \mu^2$ can be identified with the VDM contribution to $G_{q/\gamma}$.

Taking moments, we have[1]

$$G_{q/\gamma}(j,Q^2) = \frac{3\alpha}{2\pi} e_q^2 \int_{\mu^2}^{Q^2} \frac{dk^2}{k^2} f(j)\, G_{q/q}(j, Q^2, k^2) \quad (10)$$

where

$$G(j) \equiv \int_0^1 dx\, x^{j-1}\, G(x) \quad (11)$$

$$f(j) = \int_0^1 dz\, z^{j-1} \left[z^2 + (1-z)^2\right]$$

$$= \frac{1}{j} - \frac{2}{j+1} + \frac{2}{j+2} \quad (12)$$

and

$$G_{q/q}(j,Q^2,k^2) = \left[\frac{\alpha_s(k^2)}{\alpha_s(Q^2)}\right]^{\frac{d_j}{2\pi b}} \quad (13)$$

The d_j are the standard valence anomalous dimensions, as defined in Ref. [14]. Performing the k^2 integral in (10) yields

$$G_{q/\gamma}(j,Q^2) = \frac{3}{2\pi} e_q^2 \frac{\alpha}{\alpha_s(Q^2)} \left[\frac{2\pi f(j)}{2\pi b - d_j}\right] \quad (14)$$

This exhibits the remarkable scaling features of the photon structure function discussed above.

It is easy to invert the moment equation via the method of Yndurian.[16] A graph of $xG_{q/\gamma}(x)$ calculated in valence approximation in QCD and in the parton model is given in Fig. 5. Good agreement is obtained with the (valence plus singlet) results of Llewellyn Smith[5] over nearly the entire range of x.

The x near 1 behavior of $G_{q/\gamma}(x)$ can be obtained more directly from a direct integration of (10), using the $x \to 1$ form for the quark structure function[14]

$$G_{q/q}(x, Q^2, k^2) = \exp\left[(3 - 4\gamma_E)\,\xi C_2\right] \cdot (1-x)^{4C_2\xi - 1} / \Gamma(4C_2\xi) \quad (15)$$

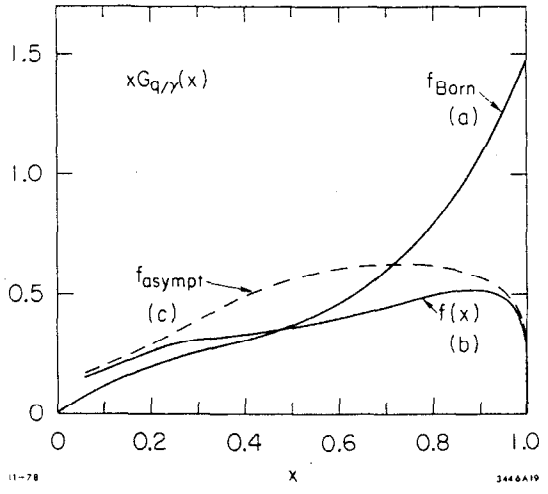

Fig. 5. The valence photon structure function $G_{q/\gamma}(x)$ as calculated in (a) Born approximation, (b) to all orders in QCD, and (c) the $x \to 1$ limit (Eq. (17)). An overall factor proportional to $\log Q^2/\Lambda^2$ is factored out (from Ref. [1]).

where $\gamma_E = 0.577...$ is Euler's constant, $C_2 = (N^2-1)/2N = 4/3$, and

$$\xi = \frac{1}{4\pi b} \ln \frac{\alpha_s(k^2)}{\alpha_s(Q^2)} \quad . \quad (16)$$

One then obtains[14]

$$G_{q/\gamma}(x,Q^2) \underset{x\to 1}{=} \frac{3}{2\pi} e_Q^2 \frac{\alpha}{\alpha_s(Q^2)} \frac{4}{4\pi b - (3 - 4\gamma_E)C_2 + 4C_2 \ln\frac{1}{1-x}} \quad (17)$$

This result is numerically accurate only for $x \gtrsim 0.97$ but is off by no more than a factor of 2 for $x > 0.1$ (see Fig. 5).

It is interesting to note that for fixed $\mathcal{M}^2$, $Q^2 \to \infty$, this expression for $G_{q/\gamma}(x,Q^2)$ approaches a constant. This implies, via the Drell-Yan relation, perfect power-law scaling for the $\gamma \to \rho$ transition form factor $F_{\gamma\rho}(Q^2) \propto Q^{-1}$.

Compared to meson distributions which fall as a power at $x \to 1$, the photon structure function is nearly flat in x, again due to the underlying $\gamma q\bar{q}$ point-like vertex. In principle the photon structure can be determined experimentally from the two photon $e\gamma \to e'X$ process, i.e.; deep inelastic scattering from a

photon target.[9]

Returning to the high p_T jet cross sections, we note the following striking fact: in each contribution to the four-jet cross section the two factors of $\alpha_s(p_T^2)$ from the subprocess cross section, e.g.,

$$\frac{d\sigma}{dt}\,(qq \to qq) \sim \frac{4\pi\left(\frac{4}{3}\,\alpha_s(t)\right)^2}{t^2} \tag{18}$$

(see Fig. 3a) actually cancel (in the asymptotic limit) the two inverse powers of $\alpha_s(p_T^2)$ from the two $G_{q/\gamma}(x,p_T^2)$ structure functions.[1] Similarly the single power of $\alpha_s(p_T^2)$ in $d\sigma/dt$ $(\gamma q \to gq)$ cancels the single inverse power of $\alpha_s(p_T^2)$ structure function in the 3-jet cross section. (See Fig. 3(b).) Thus miraculously <u>all</u> of these jet trigger cross sections obey <u>exact</u> Bjorken scaling

$$E\,\frac{d\sigma}{d^3p}\,(\gamma\gamma \to \text{Jet} + X) \underset{p_T^2 \to \infty}{\Longrightarrow} \frac{1}{p_T^4}\,f(x_T\,,\,\theta_{cm}) \tag{19}$$

when the leading QCD perturbative corrections to all orders are taken into account.[17] Furthermore, the asymptotic cross sections are even independent of $\alpha_s(p_T^2)$! The asymptotic prediction thus has essentially zero parameters.

Quite detailed numerical predictions can be made for the ee → ee Jet + X cross sections by computing $G_{q/e}$ (from the convolution of the equivalent photon approximation $G_{\gamma/e}$ and the photon structure function $G_{q/\gamma}$), and then summing in Eq. (7) over all 2-2 hard scattering QCD processes, including all quark colors and flavors. In our calculations[1] we have found it useful to display approximate analytic forms which have the correct power-law dependence at large p_T and at the edge of phase space ($x_R = 2p_J/\sqrt{s} \to 1$). The analytic forms usually agree with the numerically integrated results to within 20%. For the analytic calculations, we have used the simplified form

$$x\,G_{q/e}(x) = e_q^2\left(\frac{\alpha}{2\pi}\,\log\,\eta\right)\frac{\alpha}{2\pi}\,F_Q(1-x) \tag{20}$$

for each quark flavor and color, where $\log\,\eta = \log\,s/4m_e^2$ if the scattered electron is not tagged. The factor F_Q which is $\sim \log\,s/4m_q^2$ if we use the Born approximation for $\gamma \to q\bar{q}$, becomes of order $1/\alpha_s(Q^2)$ when the QCD radiative corrections are taken into account. We have found empirically that the value

$\alpha_s(Q^2)F_Q \tilde{=} 0.8$ gives a good characterization of the QCD normalization. [For $x \to 1$ $G_{q/e}$ actually falls as $(1-x) \log 1/(1-x)$.] Note also that for $x \to 1$, the quark and electron tend to have the same helicity.

For the 4-jet cross section, the sum over all types of jet triggers near 90^o gives

$$E \frac{d\sigma}{d^3p_J}(e^+e^- \to e^+e^- \text{ Jet} + X) \tilde{=} \left(\frac{\alpha}{2\pi} \log \eta\right)^2 \left[\frac{\alpha}{2\pi} F_Q \alpha_s(p_T^2)\right]^2 \cdot \left[80\left(\sum_f e_f^2\right)^2 + \frac{52}{9}\left(\sum_f e_f^4\right)\right] \frac{(1-x_R)^3}{p_T^4}$$

$$= 0.8 \times 10^{-2} \text{ nb GeV}^2 \frac{(1-x_R)^3}{p_T^4} \quad [\sqrt{s} = 30 \text{ GeV}] . \quad (21)$$

The sum f is over contributing quark flavors. The subprocesses include $qq \to qq$, $q\bar{q} \to q\bar{q}$, and $q\bar{q} \to gg$.

For the 3-jet events, the subprocesses $\gamma q \to gq$ and $\gamma\bar{q} \to g\bar{q}$ yield the cross section

$$E \frac{d\sigma}{d^3p_J}(e^+e^- \to e^+e^- \text{ Jet} + X) \tilde{=} \alpha\left(\frac{\alpha}{2\pi} \log \eta\right)^2 \left[\frac{\alpha}{2\pi} F_Q \alpha_s(p_T^2)\right] \cdot \left[40 \sum_f e_f^4\right] \frac{(1-x_R)^2}{p_T^4}$$

$$\tilde{=} 2.5 \times 10^{-2} \text{ nb GeV}^2 \frac{(1-x_R)^2}{p_T^4} \quad [\sqrt{s} = 30 \text{ GeV}] . \quad (22)$$

The corresponding result for the two jet cross section from $\gamma\gamma \to q\bar{q}$ is

$$E \frac{d\sigma}{d^3p_J}(e^+e^- \to e^+e^- \text{ Jet} + X) \tilde{=} 3 \times 10^{-2} \text{ nb GeV}^2 \frac{(1-x_R)}{p_T^4} , \quad (23)$$

i.e.: in general, $\sigma(2 \text{ jet}) > \sigma(3 \text{ jet}) > \sigma(4 \text{ jet})$. It is clear that there is no double counting of cross sections here since each type of jet cross section has a distinctive topological structure and different pattern of q, $\bar{q}$ and g jets.

A graph of these cross sections is shown in Fig. 6.

To remind ourselves how critical the pointlike photon couplings are to these results, let us estimate the contribution to high p_T jet production when both photons are meson dominated. We have ($f_\rho^2/4\pi \tilde{=} 2$)

$$d\sigma^{VDM}(\gamma\gamma \to \text{Jet}+X) = \left(\frac{e}{f_\rho}\right)^4 d\sigma(\rho\rho \to \text{Jet}+X)$$

$$\tilde{=} \left(\frac{4\pi\alpha}{f_\rho^2}\right)^2 \left(\frac{2}{3}\right)^2 \frac{d\sigma(pp \to \text{Jet}+X)}{(1-x_R)^4} \quad (24)$$

since we expect $G_{q/p} \sim (1-x)^2 G_{q/\rho}$. If we take $Ed\sigma\,(pp \to \text{Jet}+X)/d^3p \sim 300 \times Ed\sigma/d^3p\,(pp \to \pi X) \sim 1.1$ nb GeV^6 $(1-x_R)^9$ p_T^{-8}, then the convolution over photon momentum distributions yields the rough estimate ($\theta_{cm} \tilde{=} 90^\circ$, $\sqrt{s} = 30$ GeV)

$$E\frac{d\sigma^{VDM}}{d^3p_J}(e^+e^- \to e^+e^- \text{Jet}+X) \tilde{=}$$

$$1.4 \text{ nb GeV}^6 \frac{(1-x_R)^7}{p_T^8}, \quad (25)$$

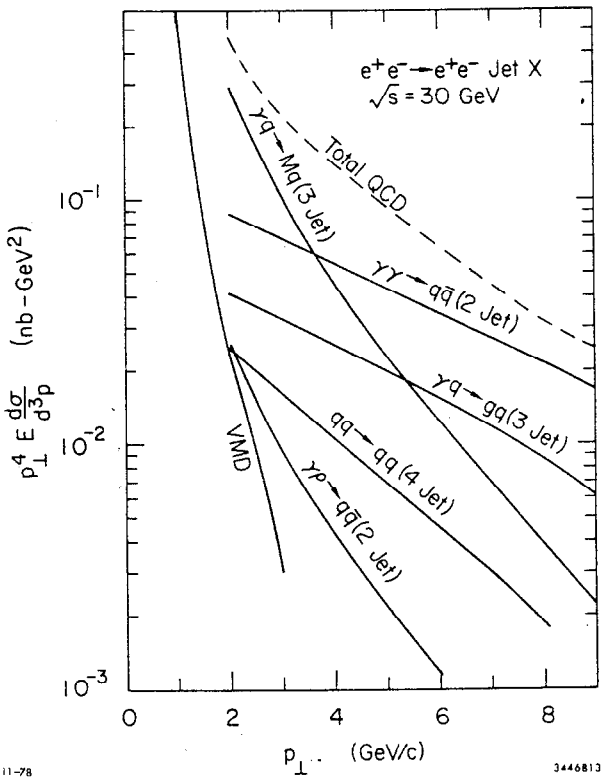

Fig. 6. QCD (and VMD) contributions to the $e^+e^- \to e^+e^-$ Jet + X. The 4-jet cross section includes the contributions from $qq \to qq$, $q\bar{q} \to q\bar{q}$, and $q\bar{q} \to gg$. (From Ref. [1]).

which is negligible compared to the pointlike contributions for $p_T > 2$ GeV (see Fig. 6). We have also checked explicitly that the QCD ($q\bar{q} \to q\bar{q}$ hard scattering) contributions from processes such as $\gamma p \to q\bar{q}\,q\bar{q}$ or $\rho\rho \to q\bar{q}\,q\bar{q}$, where one or both photons are meson dominated, are also small.

The overall scaling properties of QCD cross sections due to specific subprocesses can be easily determined from counting rules:[18]

$$E\frac{d\sigma}{d^3p}(A+B \to C+X) \tilde{=} \frac{f(\theta_{cm})}{(p_T^2)^{n_{active}-2}}(1-x_R)^{2n_{spect}^{bnd}+n_{fm}-1} \quad (26)$$

where n_{active} is the number of elementary fields (q, e, γ, g, etc.) participating in the hard scattering subprocess,[3] n^{bnd}_{spect} is the number of bound spectators, i.e.: the number of constituent fields which do not interact (and thus "waste" the incident energy),[19] and n_{fm} are the number of unbound spectator fermions (q,e) from pair production or bremsstrahlung scattering processes, as in the equivalent photon approximation. In Eqs. (21-23) the number of active fields in each case is 4; $n^{bnd}_{spect} = 0$, and $n_{fm} = 4,3$, and 2 respectively. The counting rules have small corrections due to logarithmic scale-breaking effects and the $\log \frac{1}{1-x}$ behavior of $G_{q/\gamma}$. (See Section VI.)

V. High p_T Meson Production in $\gamma\gamma$ and pp Collisions

We have also considered in some detail background contributions to the $\gamma q \to$ Jet + X cross section from (higher "twist") subprocesses that involve more than the minimum number of active fields in the hard scattering subprocess.[20] The most significant background comes from subprocesses of the form (see Fig. 7)

$$\gamma\bar{q} \to Mq$$

where a photon from one beam photoproduces a meson at large p_T on a quark constituent of the other beam. The meson trigger, the recoil quark jet, and the spectator $\bar{q}$ jet together provides a background to the $\gamma\gamma \to$ 3 jet events. The normalization of the $\gamma q \to Mq$ amplitude can be inferred in a straightforward way from $\gamma p \to \pi^+ n$ photoproduction at large momentum transfer: (see Fig. 7(b))

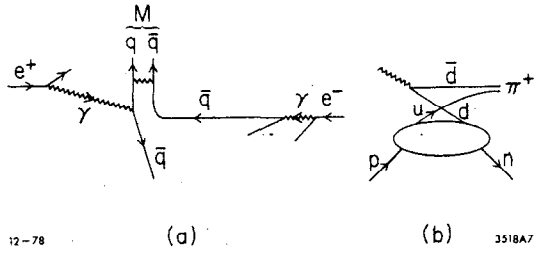

Fig. 7. Contribution of the $\gamma q \to Mq$ subprocesses to (a) $e^+e^- \to e^+e^-\pi^+X$ and (b) $\gamma p \to \pi^+ n$.

$$\frac{d\sigma}{dt}(\gamma p \to \pi^+ n) \propto F_p^2(t)\,\frac{d\hat{\sigma}}{dt}(\gamma q \to \pi q) \qquad (27)$$

The 90° exclusive cross section[21] falls as $s^{-7.3 \pm 0.4}$ in agreement with the s^{-7} behavior predicted by Eq. (27), and dimensional counting,[3] so this procedure seems justified. The net result is ($n_{active} = 5$) $E\frac{d\sigma}{d^3p}(e^+e^- \to e^+e^-$ Jet+X) = 1.1 nb GeV^4 $(1-x_R)^2/p_T^6$ where the sum over all pseudo-scalar and vector meson $q\bar{q}$ bound states in the $\underline{35}+\underline{1}$ representation of SU(3) constitutes the "jet" trigger. As shown in Fig. 6, this contribution falls faster in p_T but at $\sqrt{s}$ =

30 GeV dominates the $\gamma q \to gq$ 3 jet cross section until $p_T^{jet} \sim 6$ GeV, and (though distinguishable by topology) it even dominates the $\gamma\gamma \to q\bar{q}$ contribution until $p_T^{jet} \gtrsim 4$ GeV.

It is possible that the normalization of the $\gamma q \to Mq$ subprocess has been overestimated; nevertheless this amplitude must occur at some level, producing a characteristic $p_T^{-6}\, f(x_R, \theta_{cm})$ cross section. The most important check of its contribution will come from single particle production at large p_T, such as $e^+e^- \to e^+e^-\pi^+X$. In the case of hard scattering processes such as $\gamma\gamma \to q\bar{q}$, $\gamma q \to gq$, and $qq \to qq$, the final state fragmentation $G_{\pi/q} \sim (1-x)$ leads to a strong suppression ($\sim 10^{-2}$) in the π^+/Jet ratio, since the quark jet must be produced at higher momentum than the trigger particle (the "trigger bias" effect).[22] For example, the leading $\gamma\gamma \to q\bar{q}$ subprocess gives

$$E\frac{d\sigma}{d^3p}(e^+e^- \to e^+e^-\pi^+X) \simeq 6\times 10^{-4}\ \text{nb GeV}^2\ \frac{(1-x_R)^3}{p_T^4} \quad . \qquad (28)$$

On the other hand, the $\gamma q \to \pi^+ q$ subprocess produces a pion at high p_T, without suppression from fragmentation:

$$E\frac{d\sigma}{d^3p}(e^+e^- \to e^+e^-\pi^+_{\text{prompt}}X) = 3\times 10^{-2}\ \text{nb GeV}^2\ \frac{(1-x_R)^2}{p_T^6} \quad . \qquad (29)$$

(Inclusion of non-"prompt" π's from resonance decay approximately doubles the production rate.) This contribution is thus predicted to dominate single pion production in the $\gamma\gamma$ process until very high p_T. With the above normalization, and in the absence of electron or positron tagging, the two-photon reaction provides a significant background to the 90° inclusive π^+ spectrum from $e^+e^- \to \gamma^* \to \pi^+ + X$ for $x_T \lesssim 0.15$ at $\sqrt{s} = 30$ GeV. (See Fig. 8.)

It will be extremely interesting to verify the normalization and especially the power law of the $\gamma\gamma \to \pi^+ + X$ cross section. The p_T^{-6} power is derived directly from the lowest order diagram for $\gamma q \to (q\bar{q})q$ where the $q\bar{q}$ system is at fixed mass; higher order QCD corrections can only modify the result by an overall logarithmic factor. The fact that the single hadron trigger is so strongly dominated by "prompt" subprocesses where the high p_T trigger is produced directly in the hard scattering subprocess rather than by quark or gluon fragmentation also is an important feature in hadron-hadron collisions. In this

case, as described in the constituent interchange model (CIM),[20] dominant subprocess contributing to the $pp \to \pi^+ X$ and $pp \to pX$ cross sections for $p_T < 8$ GeV are expected to be the prompt hard-scattering reactions such as $qM \to qM$ and $qB \to qB$, respectively. These sub-processes immediately explain why the observed power law for $Ed\sigma/d^3p$ at fixed x_T and θ_{cm} are close to p_T^{-8} (meson production) and p_T^{-12} (proton production) for data below $p_T = 8$ GeV. The CIM approach also can account for the observed angular distributions, same side momentum correlations, and charge correlations (flavor transfer) between opposite sides.[23]

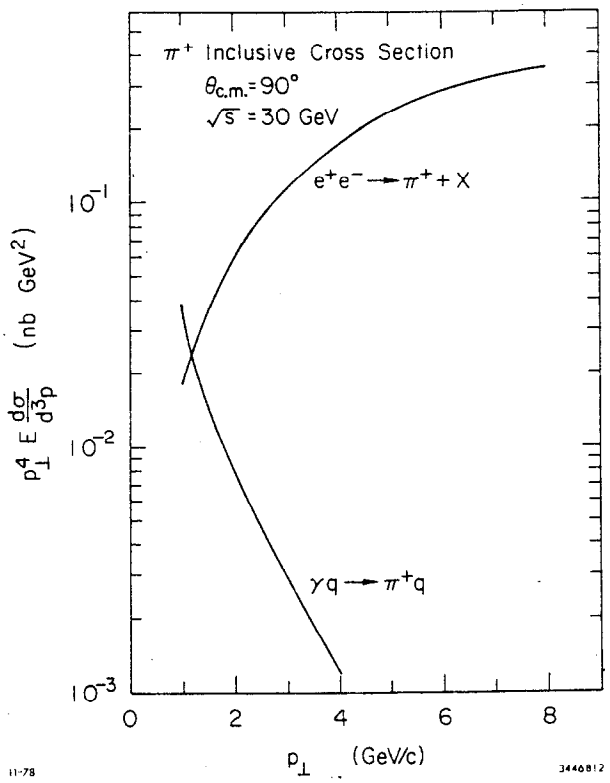

Fig. 8. Leading contributions to inclusive pion contributions from e^+e^- annihilation and $e^+e^- \to e^+e^-\pi^+X$ (from Ref. [1]).

Above $p_T > 8$ to 10 GeV, the standard $\alpha_s^2(p_T^2)p_T^{-4}$ contributions to $pp \to \pi X$ from quark or gluon QCD hard scattering processes are expected to dominate the faster falling prompt processes. The essential distinction between these competing mechanisms is simply whether the trigger hadron is formed before or after the hard scattering occurs. Both mechanisms of course occur in QCD.

Recently there have been attempts to modify the QCD quark and gluon scattering predictions by attributing strong scale violating effects to parton transverse momentum integrations.[24] However, these effects turn out to be unimportant above $p_T \gtrsim 4$ GeV when covariant off-shell kinematics are included;[25] futher this approach fails to explain (a) the p_T^{-12} scaling behavior for $pp \to pX$, (b) the small increase of same side momentum observed as p_T increases,[26] and (c) the strong charge correlations between K^- and $\bar{p}$ triggers and away side charged particles.[26] The combined CIM + QCD approach, however, does not have any of these difficulties.[23] The large jet cross sections observed in pN collision cannot be accounted for by the prompt processes alone and thus give

some support for the existence of quark and gluon hard scattering subprocesses.[27]

VI. Photon and Hadron Structure Functions at Large x and Generalized Counting Rules

It is interesting to contrast the anti-scaling form for the photon structure function $G_{q/\gamma}(x,Q^2) \sim (\alpha/\alpha_s(Q^2))f(x)$ with the large x behavior of hadronic structure functions which can be deduced from perturbative QCD. In the following I would like to give a preliminary report of some results recently obtained in collaboration with G. Peter Lepage.[28] For the discussion of violation of scale invariance, one can represent the proton structure function as a convolution (see Fig. 9)

$$G_{q'/p}(x, Q^2) = \sum_q \int_x^1 \frac{dz}{z} G^o_{q/p}(z)\, G_{q'/q}\left(\frac{x}{z}, Q^2, \mu^2\right) \qquad (30)$$

where $G^o_{q/p}$ is the structure function for constituent quarks in the nucleon derived from the bound state equation. By definition, all real and virtual gluon bremsstrahlung corrections are included in $G_{q'/q}(x,Q^2,\mu^2)$ the probability (at probe mass Q) of finding a bare quark q' in a dressed quark q of mass μ. The moments of $G_{q'/q}$ are given by the standard QCD formulae, as in Eq. (13). For $x \to 1$,[14]

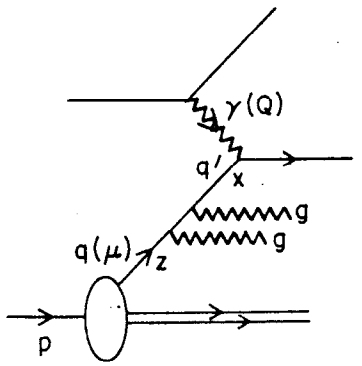

11-78 3518A9

Fig. 9. Representation of the proton structure function and QCD radiative corrections in deep inelastic lepton-proton scattering.

$$G_{q/q}(x,Q^2,\mu^2) \sim (1-x)^{\tilde{\xi}-1} P(\tilde{\xi}) \qquad (31)$$

where

$$\tilde{\xi} = 4C_2\, \tilde{\xi}(Q^2,\mu^2) \equiv \frac{4}{3\pi} \int_{\mu^2}^{Q^2} \frac{d\ell^2}{\ell^2} \alpha_s(\ell^2) \qquad (32)$$

and

$$P(\tilde{\xi}) = e^{\left(\frac{3}{4} - \gamma_E\right)\tilde{\xi}}\, \Gamma(\tilde{\xi}) \quad . \qquad (33)$$

Eq. (30) can be justified if one retains the leading logarithm in each order of perturbation theory. The value of μ^2, the off-shell constituent quark mass squared, is the mean value obtained after integration over the transverse momentum in the wavefunction. At asymptotic Q^2, $\tilde{\xi} \sim \log\log Q^2/\Lambda^2$, and the structure function contracts toward small x.

In order to compute $G^o_{q/p}(x)$, we will assume that at low momentum transfer the proton can be represented as a bound state of three quarks which approximately share the nucleon's 4-momentum. The high momentum transfer of the structure function is then controlled by the Bethe-Salpeter kernel; asymptotically one finds that the minimal gluon exchange amplitude dominates, and thus[28]

$$G^o_{q/p}(x) \propto \frac{1}{1-x}\left(\frac{\alpha_s(\mu_x^2)}{\mu_x^2}\right)^4 \underset{x\to 1}{\sim} (1-x)^3 \log^{-4}\left(\frac{1}{1-x}\right) \qquad (34)$$

where $\mu_x^2 \sim 0(-M^2/(1-x))$ gives the scale of the off-shell quark and gluon propagators. The convolution (30) then yields

$$G_{q/p}(x,Q^2) \underset{x\to 1}{\sim} \log^{-4}\left(\frac{1}{1-x}\right)(1-x)^{3+\tilde{\xi}(Q^2,\mu_x^2)} P(\tilde{\xi}) \quad . \qquad (35)$$

It is important to note that the lower limit in the $\tilde{\xi}$ integration is μ_x^2 and that the struck quark is forced far off-shell for $x\to 1$. We thus distinguish two limits:

(1) Fixed x, $Q^2\to\infty$ (Bjorken limit). In this case, $\tilde{\xi} \sim 0(\log\log Q^2)$ and the structure function contracts to $x\to 0$.

(2) Fixed $\mathcal{M}^2 = \frac{(1-x)Q^2}{x}$, $Q^2 \to \infty$ (exclusive, Bloom-Gilman limit). In this case

$$\tilde{\xi}(Q^2,\mu_x^2) \to 0\left(\frac{1}{\log Q^2}\right)$$

and hence

$$G_{q/p}(x,Q^2) \to G^o_{q/p}(x) \sim (1-x)^3\log^{-4}\left(\frac{1}{1-x}\right) \qquad (36)$$

i.e.: the QCD radiative corrections to the hadron structure function vanish! Physically, this is because for $x\to 1$, the struck quark has an off-shell mass of the same order as the probe momentum $\sqrt{Q^2}$.

Thus, contrary to usual expectations, the fixed Q^2, $x \to 1$ behavior of hadronic structure functions is controlled by the hadronic wavefunction, and is not modified by QCD radiative corrections. Further, because of their sensitivity to the $x \sim 1$ region, the large-n moments of $G_{q/H}(x,Q^2)$ at fixed Q^2 become scale invariant as $n \to \infty$. The general result for the structure function of a hadron with n_H constituent fields is

$$G_{q/H}(x,Q^2) \sim (1-x)^{2n_s-1} \log^{-2n_s}\left(\frac{1}{1-x}\right) \text{ (fixed } \mathcal{M}^2 \text{ limit)} \qquad (37)$$

(n_s = number of bound spectators = $n_H - 1$). This has a smooth exclusive-inclusive (Drell-Yan) connection with the corresponding asymptotic (spin-averaged) form factor

$$F_H(t) \sim \left[\alpha_s(t)/t\right]^{n_H-1} . \qquad (38)$$

These results give the asymptotic QCD modifications to dimensional counting rules.[3,19]

The spectator counting rule (37) for hadronic structure functions allows us to write down modified counting rules for large p_T cross sections which take into account scaling violations in the active subprocess ab → cd matrix element and the $\tilde{\xi}$ dependence of the structure functions. The leading analytic dependence for large p_T and $x_R \to 1$ at $\theta_{cm} \sim \pi/2$ for hadronic reactions A+B → C+X is[28,29]

$$E\frac{d\sigma}{d^3p}(A+B \to C+X) \sim \left(\frac{\alpha_s(p_T^2)}{p_T^2}\right)^{n_{active}-2}$$

$$\cdot (1-x_R)^{2n_s-1} \log^{-2n_s}\left(\frac{1}{1-x_R}\right) \prod_{j=a,b,c} (1-x_R)^{\tilde{\xi}_j} P(\tilde{\xi}_j) \qquad (39)$$

where n_s is the total number of spectator fields in $A \to a$, $B \to b$, and $c \to C$, and

$$\tilde{\xi}_j = \begin{cases} 0 \text{ if } j = \text{hadron}, \\ \tilde{\xi}(p_T^2, \mu_{x_R}^2) \text{ if } j = \text{quark} \\ 9/4\ \tilde{\xi}(p_T^2, \mu_{x_R}^2) \text{ if } j = \text{gluon} \end{cases} \qquad (40)$$

Again, we emphasize that the $\tilde{\xi}$ corrections become negligible in the $x_R \to 1$ fixed p_T limit. The normalization constant is derived in Ref. [12] and [1].

VII. Conclusions

In summary, it becomes evident that two photon collisions can provide a clean and elegant testing ground for perturbative quantum chromodynamics. The occurrence of $\gamma\gamma$ reactions at an experimentally observable level implies that the entire range of hadronic physics which can be studied, for example, at the CERN-ISR can also be studied in parallel in $e^{\pm}e^{-}$ machines. Although low p_T $\gamma\gamma$ reactions should strongly resemble meson-meson collisions, the elementary field nature of the photon implies dramatic differences at large p_T. We have especially noted the sharp contrasts between hadron-and photon-included reactions due to the photon's pointlike coupling to the quark current and the ability of a photon to give nearly all of its momentum to a quark. The large momentum transfer region can be a crucial testing ground for QCD since not only are a number of new subprocesses accessible ($\gamma\gamma \to q\bar{q}$, $\gamma q \to gq$, $\gamma q \to Mq$, deep inelastic scattering on a photon target) with essentially with no free parameters, but most important, one can make predictions for a major component of the photon structure function directly from QCD. We also note that there are open questions in hadron-hadron collisions, e.g., whether non-perturbative effects (instantons, wee parton interactions) are important for large p_T reactions.[30] Such effects are presumably absent for the perturbative, pointlike interactions of the photon. We also note that the interplay between vector-meson-dominance and pointlike contributions to the hadronic interactions of photon is not completely understood in QCD, and $\gamma\gamma$ processes may illuminate these questions.

ACKNOWLEDGEMENTS

I wish to thank G. P. Lepage, R. Blankenbecler, T. DeGrand, J. Gunion, J. Bjorken, and Y. Frishman for helpful conversations. I am also grateful to M. Baker and S. Ellis, the organizers of this memorial colloquium, for their warm hospitality.

FOOTNOTES AND REFERENCES

[1] S. J. Brodsky, T. A. DeGrand, J. F. Gunion, and J. H. Weis, Phys. Rev. Lett. 41, 672 (1978); and SLAC-PUB-2199 (submitted to Phys. Rev.).

[2] J. D. Bjorken and E. A. Paschos, Phys. Rev. 185, 1975 (1969).

[3] S. J. Brodsky and G. Farrar, Phys. Rev. Lett. 31, 1153 (1973); Phys. Rev. D11, 1309 (1975); V. A. Matveev, R. M. Muradyan, and A. N. Tavkheldize, Lett. Nuovo Cimento 7, 719 (1973).

[4] For a comprehensive review of the vector meson dominance model, see T. H. Bauer, R. D. Spital, F. M. Pipkin, and D. R. Yennie, Rev. Mod. Phys. 50, 261 (1978).

[5] S. J. Brodsky, T. Kinoshita, and H. Terazawa, Phys. Rev. D4, 1532 (1971). For reviews see V. M. Budnev et al., Phys. Reports 15C (1975); H. Terazawa, Rev. Mod. Phys. 45, 615 (1973); and the reports of S. Brodsky, H. Terazawa, and T. Walsh in the Proceedings of the International Colloquium on Photon-Photon Collisions, published in Supplement au Journal de Physique, Vol. 35 (1974). See also, G. Grammer and T. Kinoshita, Nucl. Phys. B80, 461 (1974); R. Bhattacharya, J. Smith, and G. Grammer, Phys. Rev. D15, 3267 (1977); J. Smith, J. Vermaseren, and G. Grammer, Phys. Rev. D15, 3280 (1977).

[6] See S. J. Brodsky et al., Ref. [5], and F. Low, Phys. Rev. 120, 582 (1960). In the case of tagged leptons $\log s/m_e^2 \to \sim\log \theta^2_{max}/\theta^2_{min}$. Derivations and more precise formula are given in Ref. [5]. An excellent discussion of the experimental considerations is given by J. Field, LEP Summer Study/1-13, October 1978.

[7] For discussion and references, see S. J. Brodsky, Ref. [5].

[8] For detailed calculations see J. Smith et al., Ref. [5], and J. Field, Ref. [6]. The $e^+e^- \to e^+e^-\tau^+\tau^-$ cross section is comparable to the $e^+e^- \to \tau^+\tau^-$ cross section at $\sqrt{s}$ = 30 GeV.

[9] S. J. Brodsky, T. Kinoshita, and H. Terazawa, Phys. Rev. Lett. 27, 280 (1971); T. F. Walsh, Phys. Lett. 36B, 121 (1971).

[10] The $\gamma\gamma \to q\bar{q}$ process for single hadron production at large p_T in e^+e^- collisions was first considered in the pioneering paper by J. D. Bjorken, S. Berman, and J. Kogut, Phys. Rev. D4, 3388 (1971). A discussion of this process for virtual γ reactions has been given by T. F. Walsh and P. Zerwas, Phys. Lett. 44B, 195 (1973).

[11] In the case of integrally-charged Han-Nambu quarks, locality of the $\gamma\gamma \to q\bar{q}$ matrix element at high p_T implies for the u,d first generation quarks

$$\mathcal{M}_{\gamma\gamma} \propto \langle 0|j^2_{em}(0)|X\rangle = \begin{cases} \sum_{c=R,Y,B} u_c^\dagger u_c\left(\frac{2}{3}\right) + d_c^\dagger d_c\left(\frac{1}{3}\right) & \left(\begin{array}{c}\text{below}\\ \text{color}\\ \text{threshold}\end{array}\right) \\ u_R^\dagger u_R + u_B^\dagger u_B + d_Y^\dagger d_Y & \left(\begin{array}{c}\text{above}\\ \text{color}\\ \text{threshold}\end{array}\right) \end{cases}$$

which aside from a sign change for the down quark is identical to the $\langle 0|j_{em}(0)|X\rangle$ matrix element. Thus, we have the identity

$$R^{HN}_{\gamma\gamma} = R$$

both below and above the color threshold. In particular, $R^{HN}_{\gamma\gamma} = \frac{5}{3} \times$ (number of flavor generations) below color threshold, and $R^{HN}_{\gamma\gamma} = 3 \times$ (number of flavor generations) above color threshold, compared to $\frac{17}{27} \times$ (number of flavor generations) for the standard QCD model. See also M. Chanowitz in "Color Symmetry and Quark Confinement", Proceedings of the 12th Rencontre de Moriond, 1977, edited by Tran Thanh Van, and P. V. Landshoff, LEP Summer Study/1-13, October 1978.

[12] Equation (6) has also been derived in an equivalent form by K. Kajantie, University of Helsinki reprint, September 1978.

[13] For a review see D. Sivers, R. Blankenbecler, and S. Brodsky, Phys. Reports 23C : 1 (1976). For a discussion of the validity of the hard scattering expansion in field theory, see W. E. Caswell, R. R. Horgan, and S. J. Brodsky, Phys. Rev. D18, 2415 (1978). Note that processes where one electron balances the transverse moment of the high p_T jet trigger also occur in (3).

[14] Yu. L. Dokshitser, D. I. Dyakanov, and S. I. Troyan, Stanford Linear Accelerator Center translation SLAC-TRANS-183, translated for Proceedings of the 13th Leningrad Winter School on Elementary Particle Physics, 1978.

[15] E. Witten, Nucl. Phys. B120, 189 (1977). The results of Witten have been rederived by summing ladder graphs by W. Frazer and J. Gunion, University of California at Davis preprint 10P10-194 (1978) and by C. H. Llewellyn Smith, Oxford preprint 67/78. See also Ref. [14].

[16] F. J. Yndurian, Phys. Lett. 74B, 68 (1978).

[17] This remarkable scaling property was first pointed out by C. H. Llewellyn Smith, Oxford preprint 56/78 (1978).

[18] See Refs. [13], R. Blankenbecler, S. J. Brodsky, and J. F. Gunion, Phys. Rev. D18, 900 (1978), and Ref. [1]. If the spin of a constituent a does not match that of the projectile A, then there is an additional suppression factor $(1-x)^{2|S_z^a - S_z^A|}$ in the leading scaling term. S. J. Brodsky, J. F. Gunion, and M. Scadron (to be published). Logarithmic QCD corrections to the power-law behavior are discussed in Section VI.

[19] S. J. Brodsky and R. Blankenbecler, Phys. Rev. D10, 2973 (1974).

[20] R. Blankenbecler, S. J. Brodsky, and J. F. Gunion, Phys. Rev. D18, 900 (1978); P. V. Landshoff and J. C. Polkinghorne, Phys. Rev. D8, 927 (1973), Phys. Rev. D10, 891 (1974).

[21] R. Anderson et al., Phys. Rev. Lett. 30, 627 (1973). For a comparison of Compton scattering and photoproduction, see M. A. Shupe et al., Cornell preprints (1978).

[22] S. D. Ellis, M. Jacob, and P. V. Landshoff, Nucl. Phys. B108, 93 (1976). See also J. D. Bjorken and G. R. Farrar, Phys. Rev. D9, 1449 (1974).

[23] For recent discussions see S. J. Brodsky, SLAC-PUB-2217, October 1978, and D. Jones and J. F. Gunion, SLAC-PUB-2157, July 1978.

[24] R. P. Feynman, R. D. Field, and G. C. Fox, CALT-68-651 (1978). See also A. P. Contogouris, R. Gaskell, and S. Papadopoulos, Phys. Rev. D17, 2314 (1978); A. P. Contogouris, McGill preprint (1978). J. F. Owens and J. D. Kimel, FSU HEP 780330 (1978); J. F. Owens, FSU HEP 780609 (1978), Phys. Lett. 76B, 85 (1978). J. Ranft and G. Ranft, preprints KMU-HEP-7806 and 7805 (1978), Nuovo Cimento Lett. 20, 669 (1979). M. Fontannaz, Nucl. Phys. B132, 452 (1978).

[25] For an extensive discussion see W. E. Caswell, R. R. Horgan, and S. J. Brodsky, Ref. [13]. Detailed calculations for QCD subprocesses are given by R. R. Horgan and P. Scharbach, SLAC-PUB-2188 (1978). The importance of off-shell kinematics in calculating k_T fluctuations has also been discussed by K. Kinoshita and Y. Kinoshita, KYUSHU-78-HE-6 (1978), M. Chase, DAMTP 77/29 (1977), R. Raitio and R. Sosnowski, HU-TFT-77-22 (1977).

[26] M. G. Albrow et al., NBI preprints (1978), presented by R. Moller to this conference, and K. H. Hansen, presented to the XIX Int. Conf. on High Energy Phys., Tokyo (1978), and Nucl. Phys. B135, 461 (1978).

[27] R. D. Field, CALT-68-683 (presented at the XIX Int. Conf. on High Energy Phys., Tokyo, 1978, and references, therein).

[28] S. J. Brodsky and G. P. Lepage (in preparation). I would also like to thank R. Blankenbecler for helpful discussions. The results in Section VI have been explicitly derived for psuedoscalar meson $q\bar{q}$ bound states. The extension to hadrons with spin given here is based on a straightforward generalization of these results, but still requires an explicit derivation. A complete report will be reported elsewhere. Equations (34), (37), and (38) can also be derived from renormalization group methods if one assumes that hadron matrix elements have no mass singularities. S. J. Brodsky, Y. Frishman, and G. P. Lepage (in preparation).

[29] See also S. J. Brodsky, Proceedings of the 1978 La Jolla Summer Institute (to be published). Related counting rules have been recently derived independently by T. DeGrand (private communication).

[30] I wish to thank J. Ellis for conversations on this point.